



**Scale-up Preparation, Column Chromatography-Free
Purification of Protected Carbonyl Containing Biomass
Molecules and Their Derivatizations**

Journal:	<i>Green Chemistry</i>
Manuscript ID	GC-ART-07-2023-002715.R1
Article Type:	Paper
Date Submitted by the Author:	24-Sep-2023
Complete List of Authors:	Huang, Lei; China University of Petroleum, Beijing, Institute of New Energy Li, Chen; China University of Petroleum Beijing An, Zhidong; China University of Petroleum Beijing, Institute of New Energy Zhang, Heqi; China University of Petroleum Beijing Vlachos, Dionisios; Univ. of Delaware, Li, Jiang; China University of Petroleum, Beijing, Institute of New Energy

ARTICLE

Scale-up Preparation, Column Chromatography-Free Purification of Protected Carbonyl Containing Biomass Molecules and Their Derivatizations

Received 00th January 20xx,
Accepted 00th January 20xx

DOI: 10.1039/x0xx00000x

Lei Huang,^{a†} Chen Li,^{a†} Zhidong An,^a Heqi Zhang,^a Dionisios G. Vlachos^{*b} and Jiang Li^{*a}

The protection strategy recently received significant attention due to improving product selectivity and process efficiency for biomass conversion. In this work, an effective route to protect the carbonyl group of biomass-based furans with 1,3-propylene glycol followed by simple but effective purification is first established. Sulfamic acid, a commercially available and low-cost heterogeneous Brønsted acid catalyst under our conditions, exhibits excellent acetalization performance at a gram level with good recyclability. Then an efficient, column chromatography-free purification protocol is established to give gram-level, high-purity acetal products by bypassing large eluent use, long times, and poor separation of strong polarity molecules by column chromatography. We further examine the protection group effect on selectivity during hydrodeoxygenation, deoxygenation, or ring hydrogenation of biomass-derived furanic compounds over supports with different acidity/basicity under reducing atmosphere that differs from previous reports usually focused on aerobic oxidation. Finally, a positive effect of protection strategy on photocatalytic oxidation of HMF is reported. Overall, our work greatly expanded the application potential of protection strategy via proposing effective scale-up preparation method for the commercial unavailable substrates and exploring more reaction types especially under reducing atmosphere. Grand blueprint to explore the protection strategy in biomass conversions can be imagined.

Introduction

The environmental concerns lead to the urgent need for the utilization of renewable biomass to produce fuels and chemicals.¹⁻⁴ Compared with current petrochemical raw materials and corresponding building blocks, biomass and its derivatives usually have a higher degree of functionalization and higher oxygen content. These oxygen-containing functional groups, such as carbonyl and hydroxyl groups, possess high reactivity and poor chemical stability, leading to significant side reactions and low product selectivity during biomass conversion.⁵ Protective chemistry common in small-scale organic synthesis is currently being intensively explored for biomass conversion, and the protection of highly active oxygenated groups leads to better selectivity. For example, Luterbacher et al. reported that the protection of β -O-4 structure by formaldehyde during the pretreatment of lignin greatly improves lignin monomer yield from 7-26% to 47-78% in hydrogenolysis (Scheme 1A).^{6,7} Formaldehyde reacts with the α,γ -diol groups in the β -O-4 structure to form 1,3-dioxane

structures, which effectively inhibit the undesired repolymerization during lignin depolymerization. They further reported that acetaldehyde and propionaldehyde are the best protective reagents.⁸ This protection strategy can also be used in lignin depolymerization in oxidation pathways⁹ and lignin valorization in endocarp biomass,¹⁰ providing unique lignin oligomers for tunable polyurethane bioresins.¹¹ The protection strategy can also improve the product selectivity during the conversion of cellulose and hemicellulose. Luterbacher and co-workers increased the sugar yield during the depolymerization of hemicellulose and cellulose by adding formaldehyde to effectively prevent the dehydration of sugars to furans and their further degradation (Scheme 1B).¹² 90% of xylose was recovered as diformylxylose vs. 16% without formaldehyde. A glucose yield >70% was achieved vs. a 28% yield without formaldehyde. This strategy can also be used to enhance the production of xylitol.¹³

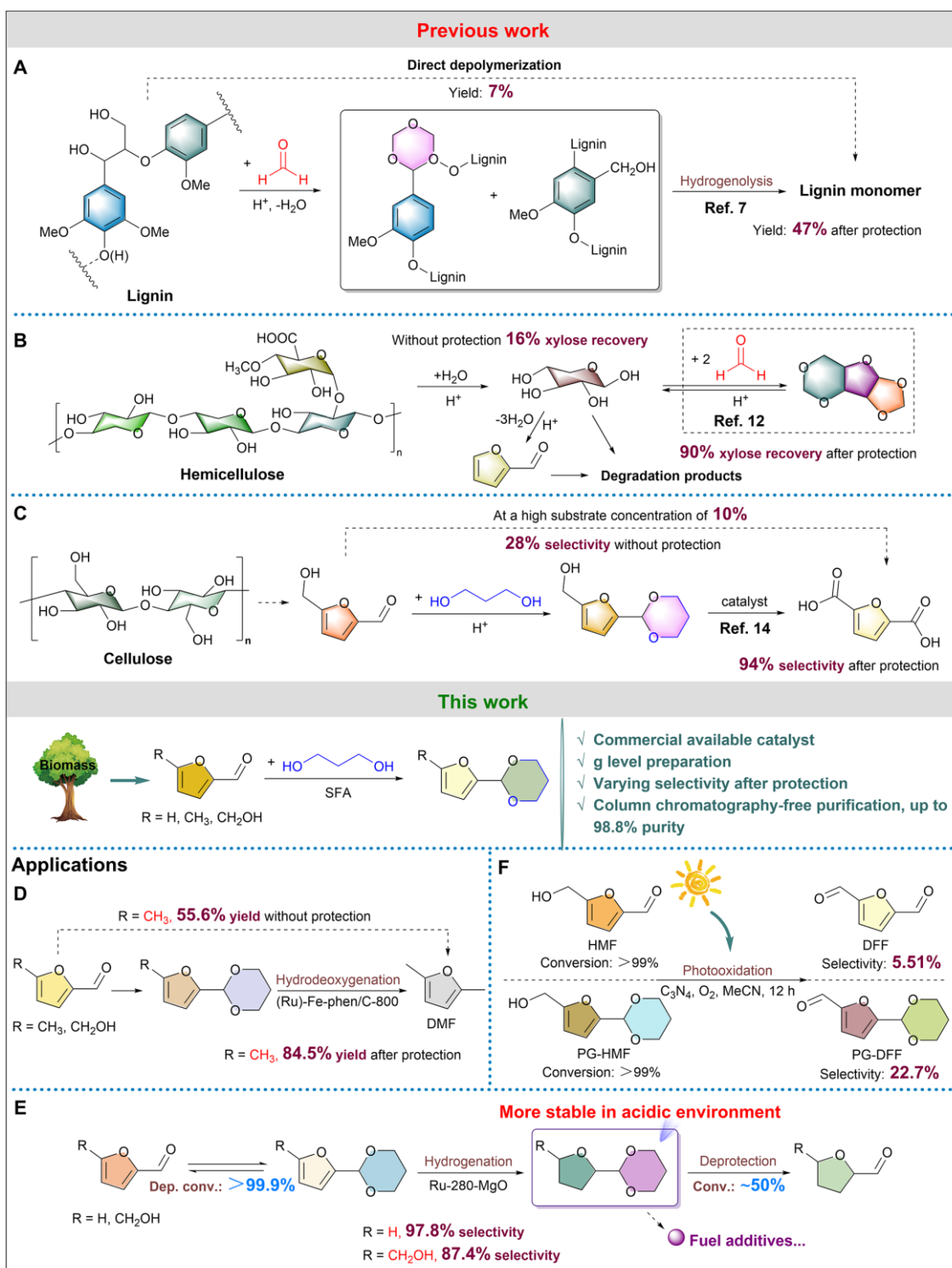
Nakajima et al. successfully realized the oxidation of concentrated 5-(hydroxymethyl)furfural (HMF) to FDCA using the protection strategy (Scheme 1C).¹⁴ 1,3-propylene glycol can protect the aldehyde group of HMF more effectively than methanol and ethylene glycol. The six-membered acetal ring prevents the thermal decomposition and self-polymerization of HMF in concentrated solutions. The protected product of HMF, PG-HMF (PG: 1,3-propylene glycol), affords 90-95% yield of furan-2,5-dicarboxylic acid (FDCA) over Au/CeO₂ at a high substrate concentration (10-20 wt%), while previous oxidation needs to operate at a concentration of 0.5-2.1 wt%. The

^a College of New Energy and Materials, China University of Petroleum (Beijing), Beijing 102249, China. E-mail: lijiang@cup.edu.cn; Fax: (+86) 010-89731300.

^b Department of Chemical and Biomolecular Engineering and Catalysis Center for Energy Innovation, University of Delaware, 221 Academy St., Newark, Delaware 19716, United State. Email: vlachos@udel.edu.

† These authors contributed equally.

Electronic Supplementary Information (ESI) available: [details of any supplementary information available should be included here]. See DOI: 10.1039/x0xx00000x



Scheme 1. Protection strategy to improve selectivity during biomass conversion.

oxidation in methanol and ethylene glycol gave 80-95% yield of dimethyl ester (MFDC) and glycol ester (HEFDC), respectively.¹⁵ In addition, a 50 wt% solution of PG-HMF (the solvent is *N,N*-dimethylformamide) can be oxidized to PG-DFF over Ru/g- Al_2O_3 with a yield of 84.0% at 94.2% conversion.¹⁶ In contrast, aerobic oxidation of non-protected HMF at a 10 wt% solution only afforded moderate yield of DFF (52.3%). A hydroxyapatite-supported Au catalyst can selectively oxidize PG-HMF in a 10 wt%

solution to PG-FFCA (5-formylfuran-2-carboxylic acid) with a yield of 94% within 2 hours at 373 K under 0.5 MPa of O_2 .¹⁷ Deprotection of PG-FFCA by mineral acids affords FFCA in 98% yield and recovers nearly all PG. Subsequently, FFCA in a 20 wt% solution can be oxidized to FDCA in 95% yield under similar reaction conditions. The hydrogenation of high concentration PG-HMF (10-20 wt%) over $\text{NiRe}_{0.5}$ catalyst at 40°C give 81-89% yield of 2,5-hydroxymethylfuran (BHMF) BHMF.¹⁸

Although protection strategy has been applied to some preliminary work about biomass depolymerization and furanic compounds conversion,^{6,7,9-13,19-22} limited reaction types are investigated yet.^{14-18,23} The effect of protection strategy is commonly investigated in an oxidative environment. In reducing atmosphere like H₂, the influence of protection strategy on hydrogenation or hydrodeoxygenation has not been systematically evaluated. In addition, photocatalysis has recently gained significant attention due to mild reaction conditions. As highly active photo-induced radicals will lead to undesirable side reactions, the potential for introducing protection strategy in photocatalytic oxidation can be imagined.²⁴⁻²⁸

In addition, acetalization is a classic, reversible, acid-catalyzed organic chemistry reaction.²⁹ The protection of biomass derivatives entails protecting either the α,γ -diol in lignin using aldehydes or the aldehyde group in furans using 1,3-propylene glycol. The protection in the former can be carried out in parallel with the acid degradation of lignin. Research on the latter is still under developing. Previous work focused on preparation of furfural or HMF-based acetals using methanol,^{30,31} ethanol,³²⁻³⁶ or glycerol³⁷ for biofuel candidates. Developing a suitable purification protocol for furan-based 1,3-propylene glycol acetal is quite essential to further develop the protection strategy because these compounds are still commercial unavailable. The column chromatography, commonly used in traditional organic synthesis, is very time- and eluent-consuming, and incapable of scale-up separating biomass-based substrates of strong polarity. Moreover, the silica gel used in the packed column is weakly acidic, leading to deprotection during purification, thereby affecting the final product purity. For example, HMF acetal's purity is variable and not as high.^{14,18} Overall, developing a highly selective catalyst and efficient purification system, as well as the exploration of novel derivatization pathways for the conversion of protected furan compounds, is essential in the protection strategy.

Here we propose an effective route to prepare 1,3-propylene glycol-based acetals of the aldehyde group of biomass-derived furans with excellent purity (Scheme 1). Sulfamic acid, a commercially available, low-cost heterogeneous Brønsted acid catalyst, catalyzes the protection at a gram level, and can be easily recycled. An efficient, column chromatography-free purification protocol is established that bypasses the waste of eluent and long times of column chromatography, giving gram-level, high-purity acetal products. Then, we explore the effect of protection strategy in hydro-deoxygenation (HDO/DO), furanic ring hydrogenation, and photocatalytic oxidation using 5-hydroxymethylfurfural (HMF), furfural and 5-methylfurfural (MF) and their acetals as model compounds (Scheme 1D-F). The acidity/basicity of the carrier influenced greatly on the product distributions. HDO, DO, and ring hydrogenation are the main pathways for the conversion of these acetals over Ru-Fe-phen/C-800, Ru-Fe-phen/Al₂O₃-800, and Ru-280-MgO catalysts, respectively. For HDO of MF, the yield of 2,5-dimethylfuran (DMF) reaches 84.5% over Fe catalysts vs. 55.6% without protection. For HMF, the HDO selectivity does not significantly improve or it even decreases. This selectivity trend is different

from that in aerobic oxidation, likely due to the different reaction pathways and active sites. After ring hydrogenation of acetals over Ru-280-MgO catalysts, their stability in acidic environment is significantly improved, showing great potential as advanced fuel additives. Finally, positive effect of the protection strategy in photocatalytic oxidation is reported. When using g-C₃N₄, the selectivity of the target product increased fourfold (22.7% vs. 5.51%) after protecting the C=O group. Overall, this work establishes a reproducible protocol for preparing gram-level, high-purity furanic acetals, paving the way for further developing the protection strategy in chemical and photochemical biomass conversion.

Results and discussion

Catalyst screening and acetalization of furfural over SFA catalyst

Various Brønsted acids with pKa ranging from -12 to 9.24 were screened for acetalization of furfural with 1,3-propylene glycol (PG) at 30 °C (Figure 1A). Trifluoromethanesulfonic acid (TFA), the strongest acid investigated in this work (pKa = -12), afforded the highest furfural conversion. However, the selectivity to acetal is quite low due to significant side reactions. The selectivity of acetal increased to >90% when the pKa of the acid ranges from -3 to 2. Acids in this range include sulfuric acid (SA), p-toluenesulfonic acid (PTSA), methanesulfonic acid (MSA), sulfamic acid (SFA), and sodium hydrogen sulfate (SHS). Weak acids, such as citric acid (CTA) and boric acid (BA), were incapable of catalyzing the acetalization, giving very low conversion of furfural and selectivity to acetal.

The appearance of representative catalysts and reaction solutions before and after acetalization is shown in Figure 1C. Using SFA, the solution remained transparent and the catalyst kept at solid, suggesting that it is a good heterogeneous acid catalyst for the acetalization. The heterogeneity of SFA is further confirmed as shown in Figure 1B. When the SFA catalyst is removed by filtration after 60 mins, the yield of acetal remains nearly unchanged in another 60 mins. The acetalization continues after re-addition of SFA catalyst with a slightly lower reaction rate due to the partial loss of catalyst during filtration. By comparison, PTSA and MSA dissolve in the solvent, and the reaction solution turns black after acetalization. The color of SHS also turns dark after the reaction. Thus, SFA is chosen as the optimal heterogeneous acid catalyst in the following sections.

The time course of the SFA-catalyzed acetalization is shown in Figure 1D. The ratio of PG/furfural is raised to 4:1 to achieve higher selectivity to acetals (the optimization of PG/furfural ratios is shown in Figure 1E). The yield of acetal achieved is 58.8% at 60.1% conversion of furfural at 30 °C after 6 h. At a higher reaction temperature of 60 °C, 93.4% yield of acetal is obtained with 97.6% conversion of furfural at 3 h. A slight decrease of furfural conversion and acetal yield are observed when the reaction time is extended to 6 h. Besides SFA, the time course of TFA, PTSA, and CTA are also recorded (Figure S1). For TFA,

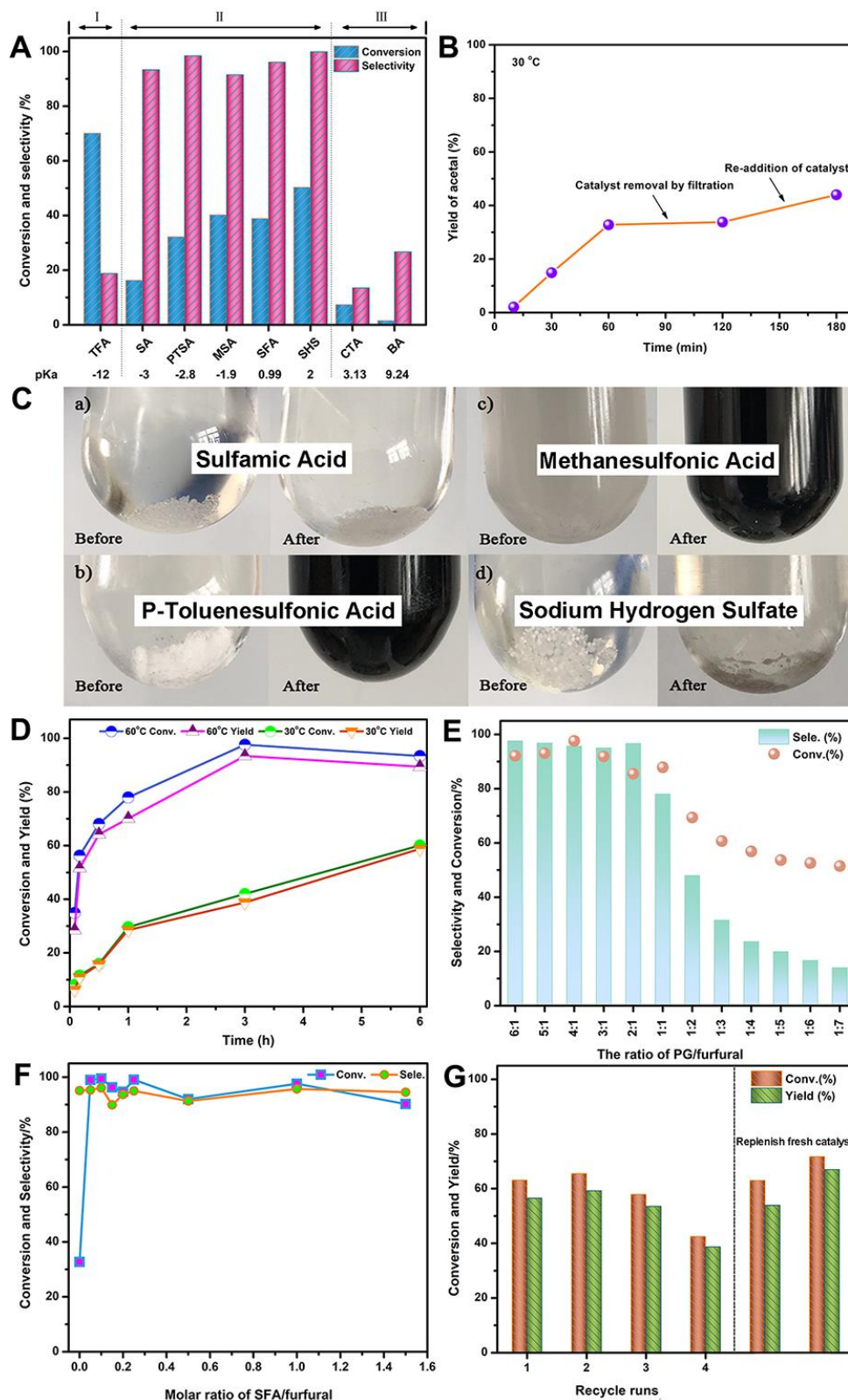


Figure 1. (A-C) Catalyst screening. A, The acetalization of furfural over various acid catalysts. Reaction conditions: 1 mmol furfural, 1 mmol 1,3-propylene glycol, 1 mmol catalyst, 3 mL dichloromethane, 30 °C, 3 h. B, Heterogeneity of SFA catalyst. C, Appearance of the catalyst and reaction solution before and after acetalization. a) SFA, b) PTSA, c) MSA, and d) SHS. (D-G) The acetalization of furfural over SFA catalyst. D, Time course. Reaction conditions: 1 mmol furfural, 4 mmol 1,3-propylene glycol, 1 mmol catalyst, 3 mL dichloromethane solvent. E, Effect of PG/furfural ratio. The conversion and selectivity are calculated based on furfural. F, Effect of SFA/furfural ratio. G, Recyclability. Reaction conditions: 1 mmol furfural, 4 mmol 1,3-propylene glycol, 0.1 mmol catalyst, 60 °C, 10 min, 3 mL dichloromethane solvent. 0.03 mmol fresh catalyst is replenished after 4th cycle.

43.7% yield of acetals is obtained at 50% conversion of furfural in only 5 min, and then the acetals yield and furfural conversion increase to 72.4% and 92.4%, respectively after 3 h. For PTSA, it is unexpected that the reaction reached equilibrium within 5

min, affording 84.6% yield of acetals at 89.3% conversion of furfural. At a higher reaction temperature of 60 °C, inferior catalytic performance is observed over these catalysts, especially TFA, suggesting that higher reaction temperature is not favorable using acids with $pK_a < -2.8$. By comparison, CTA ($pK_a = 3.13$) shows similar reaction trends to SFA but inferior performance.

The effect of the ratio of PG/furfural on performance is investigated in Figure 1E. At a ratio of 1:1, 78% selectivity of acetals is obtained at 87.9% conversion of furfural at 60 °C in 3 h. This selectivity is lower than that obtained at 30 °C. The selectivity of acetals significantly decreases with decreasing ratio of PG/furfural because furfural is unstable in an acidic environment.³⁸ Thus, excessive PG is favorable for the acetalization, and the optimal PG/furfural ratio of 4:1 affords 97.6% conversion of furfural and 95.7% selectivity of acetals.

As SFA is a heterogeneous acid catalyst under our acetalization conditions, the same amount of SFA as furfural is added first and the catalyst loading is then investigated (Figure 1F). The catalyst loading can be decreased to 5%, giving 99% conversion of furfural and 95.3% selectivity to acetals. In the absence of SFA, the conversion of furfural significantly dropped to 32.7%, i.e., the Brønsted acid catalyst is important.

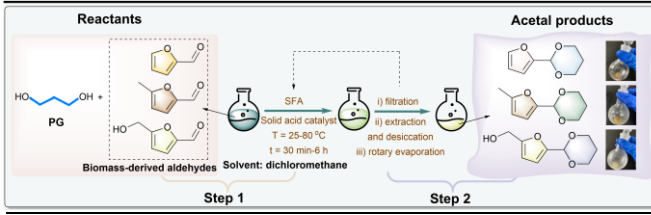
Finally, the reusability of SFA is examined in six consecutive cycles under conditions giving moderate furfural conversion (Figure 1G). A decrease in the catalytic performance is observed after the 3rd run, probably due to the catalyst loss during the catalyst recovery. Thus, 3 mg of fresh catalyst (ca. 30% of the initial catalyst) is replenished after the 4th run, and the catalytic activity is successfully recovered to the initial level.

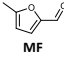
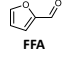
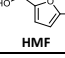
Scale-up preparation and purification

Having established a robust acid catalyst for the acetalization of furfural with PG, we next turn to the scale-up of the acetalization of several biomass-derived aldehydes. Excellent performance is still observed at a scale of 10 mmol, affording 97.8% conversion of furfural and 93.5% yield of acetals. The conversion of HMF is lower than that of furfural, suggesting that the reaction equilibrium shifts more to the reactants, consistent with a previous report.¹⁴

Another key concept in scale-up is the purification of acetals without using column chromatography, which is unsuitable for large-scale production. After trials, a practical route is finally established, as shown in Table 1. The acid catalyst is first separated from the mixture by filtration, and then PG is separated by extraction using water or a saturated brine. For furfural, water leads to a slightly higher isolated yield and purity of acetals. In contrast, very low isolated yields of HMF-derived acetals are obtained using water, and the isolated yield is significantly increased to 57.5% using a saturated brine. The additional –OH group in HMF significantly increases its molecular polarity, leading to a lower partition coefficient between CH_2Cl_2 and water.³⁹ Thus, more HMF and HMF-derived acetals are present in the aqueous phase when water is used for extraction, leading to a significantly lower isolated yield. Therefore, a saturated brine is required for HMF-based acetals. Finally, pure acetals are obtained by rotary evaporation of the

Table 1. Scale-up preparation and purification of acetals from various biomass-derived aldehydes.



Substrate	Mol./mmol	Step 1		Step 2	
		GC Conv./%	GC Yield/%	Isolated Yield (Purity)/%	
				Deionized water	Saturated brine
 MF	10	94.7	91.4	63.2(94.1)	78.7(98.8)
 FFA	10	97.8	93.5	76.4(96.0)	73.7(93.9)/71.1(90.0) ^a
 HMF	10	89.3	88.1	5.9(91.1)	57.5(98.6)/60.2(90.9) ^a

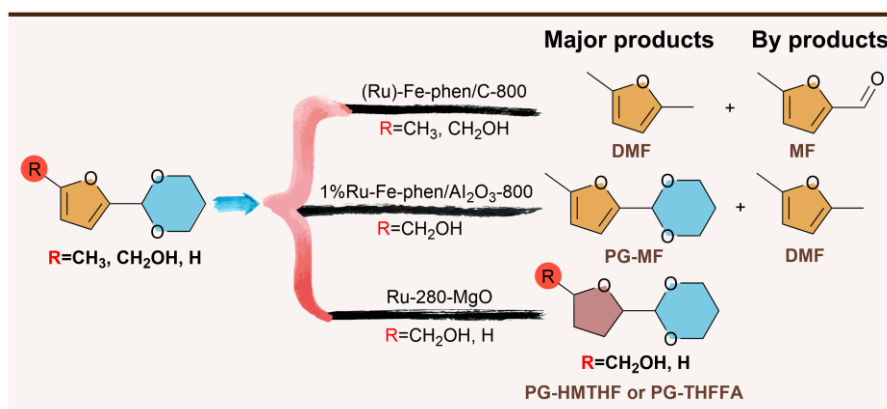
^a Scale-up and purification of acetals from 50 mmol FFA or HMF at enhanced substrate concentration.

organic phase after desiccation (see Figure S9 for a clearer view). The ¹H NMR spectra of the furfural-derived acetals after the column chromatography or using our protocol are nearly the same, further confirming that our protocol effectively purifies the acetals. All GC and ¹H NMR spectra are shown in Figures S3-S8. The process is further operated at a larger scale of 50 mmol with a three times higher substrate concentration than that at a scale of 10 mmol using furfural or HMF as the substrates. Very low isolated yields are obtained when using water during extraction due to emulsification. Thus, saturated brine is more suitable for the extraction, and the isolated yield of furfural and HMF-derived acetals at 50 mmol scale can be obtained similar to those at a 10 mmol scale, with purity of ca. 90%.

Protection group effect in HDO reactions

The reactivity of aldehydes and corresponding acetals is first compared in HDO reactions over Fe and RuFe catalysts (Table 2). Previously we have reported the first example of Fe-catalyzed HDO of HMF, with the hydrogenation of the C=O group being the rate-determining step.⁴⁰ To explore the protection group effect, MF is used as a model compound, and a 55.6% yield of DMF is attained at 60.3% conversion (entry 1). After protecting the C=O group, the conversion of the substrate significantly increases to >99.9%, and DMF yield is 84.5%. Meanwhile, 10.7% MF is obtained by deprotection (entry 2). Thus, the Fe-catalyzed HDO of C=O group is significantly improved upon protecting the C=O group.

The HDO of HMF gave 32.7% yield of DMF and 44.1% yield of MF, suggesting that the additional –OH group decelerated the HDO reaction over the Fe catalyst (entry 3). The HMF-derived acetals just gave slightly higher yield of DMF than HMF (entry 4). As the Fe catalyst is incapable of catalyzing HDO at higher concentrations, we further prepared bimetallic RuFe catalysts to investigate the protection group effect in concentrated

Table 2. Protection group effect in hydrodeoxygenation (HDO), deoxygenation (DO), or ring hydrogenation reactions.^a

Entry	Catalyst	Substrate	Conv./%	Selectivity /%			
				DMF	MF	PG-MF	PG-M ^d
1	Fe-phen/C-800	MF	60.3	92.2	-	-	-
2	Fe-phen/C-800	PG-MF	>99.9	84.5	10.7	-	-
3	Fe-phen/C-800	HMF	>99.9	32.7	44.1	-	-
4	Fe-phen/C-800	PG-HMF	>99.9	37.8	37.8	-	-
5	1%Ru-Fe-phen/C-800	MF	>99.9	79.7	-	-	-
6	1%Ru-Fe-phen/C-800	PG-MF	>99.9	91.4	-	-	-
7	1%Ru-Fe-phen/C-800	HMF	>99.9	88	-	-	-
8	1%Ru-Fe-phen/C-800	PG-HMF	>99.9	87.8	-	-	-
9	1%Ru-Fe-phen/Al ₂ O ₃ -800	HMF	>99.9	62.3	-	-	-
10	1%Ru-Fe-phen/Al ₂ O ₃ -800	PG-HMF	50.2	14.5	-	71.5	-
11 ^b	1%Ru-Fe-phen/Al ₂ O ₃ -800	PG-HMF	71.0	14.4	-	73.8	-
12	Ru-280-MgO	PG-HMF	53.8	-	-	-	87.4
13	Ru-280-MgO	PG-FFA	73.9	-	-	-	89.9
14 ^c	Ru-280-MgO	PG-FFA	77.5	-	-	-	97.8

^a Reaction conditions: 0.5 mmol substrates, 100 mg catalyst, 20 mL THF, 240 °C, 12 h, 4 MPa H₂; entries 9-14, 160 °C, 2 h. ^b Additional 0.05 mmol NaHCO₃. ^c 20 mL n-hexane. ^d PG-M: PG-HMTHF or PG-THFFA when HMF or furfural is used as substrate, respectively.

solution. For MF, the yield of DMF is enhanced from 79.7% to 91.4% after protecting C=O, suggesting a positive protection group effect (entries 5 and 6). For HMF, the results are similar (entries 7 and 8), and negative protective effect is found at higher substrate loadings (Table S1). Such an effect is different from Nakajima's report for HMF oxidation, where a positive protective effect was observed at a higher concentration of HMF.¹⁴ The difference is first attributed to the reaction type. Highly active and unstable species such as radicals could form during aerobic oxidation, and their concentration may be kept low after protecting C=O. In contrast, the HDO reaction is performed in a reductive atmosphere, and the intermediate alcohols are more stable under reaction, weakening the protection group effect. An additional deprotection step may be required when acetals are used, so inferior performance is observed, especially at higher substrate loadings.

As the deprotection of acetals can be achieved in acidic environment, we also tried to use acidic support Al₂O₃-based catalysts for the HDO reactions. The conversion of HMF affords 62.3% yield of DMF (entry 9). After protecting the C=O group, the main product turns to PG-MF with 71.5% selectivity at a conversion of 50.2% (entry 10). Thus, deoxygenation, rather than hydrodeoxygenation, is more dominant, and the acetals groups are still preserved under reducing atmospheres. The

addition of base like NaHCO₃ significantly improves the conversion (entry 11), but the selectivity is still unchanged.

When Ru-280-MgO is used, ring hydrogenation turns to the major reaction pathway, giving 87.4% selectivity of PG-HMTHF or 89.9% selectivity of PG-THFFA as the major products from PG-HMF or PG-FFA, respectively (entries 12 and 13). Since Al₂O₃, MgO, and C are widely known as acidic, basic, neutral supports, respectively, NH₃- and CO₂-TPD of Ru-supported catalysts are further examined to analyze their acidity and basicity (Figure S10). Strangely, the NH₃- and CO₂-TPD profiles are similar for all Ru catalysts. We speculated that the signals may be mainly related to unstable gaseous compounds generated from Ru-catalyzed decomposition, consistent with the mass loss in TGA profile (Figure S11). The selectivity of PG-THFFA can be further improved to 97.8% at a lower temperature (160 °C) in n-hexane for 2 h (entry 14).

Afterwards, when we evaluate the deprotection of the above acetals, we found that the acetals became more stable after hydrogenation of the furanic ring. Under same deprotection conditions (0.01 mol/L HCl aqueous solution and stirring for 30 seconds at room temperature), 91.6% conversion of PG-FFA was achieved while the conversion of PG-THFFA is only ca. 50% (Figure 2). As PG-FFA has been recommended as fuel additives,^{37, 41-43} the better stability of PG-THFFA holds great

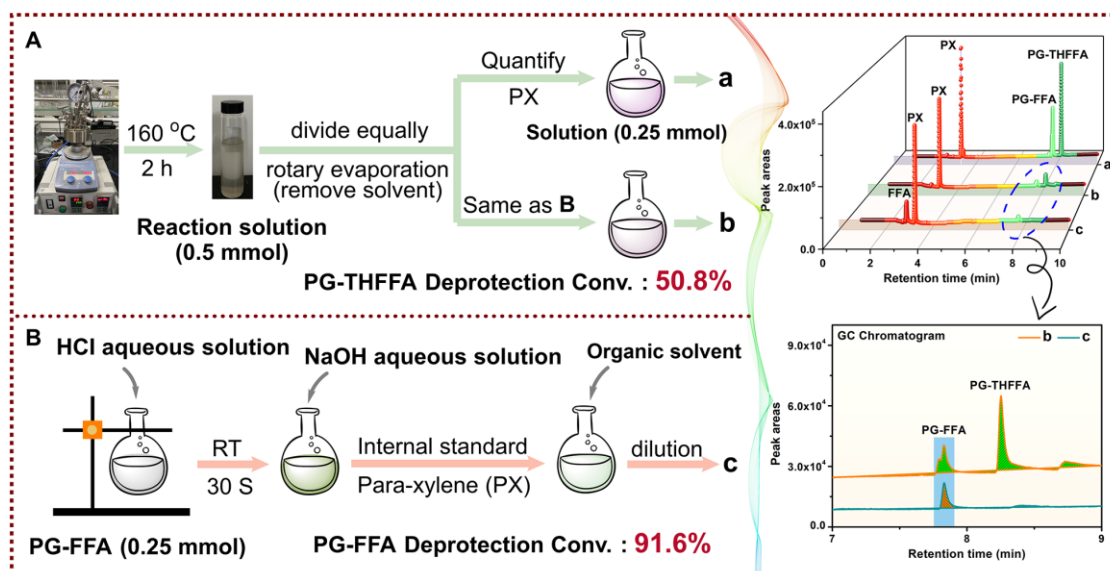


Figure 2. Examination of the stability of acetals under acidic environment. **A**, Reaction steps for deprotection of PG-THFFA. **B**, Reaction steps for deprotection of PG-FFA. PG-THFFA is obtained from ring hydrogenation of PG-FFA.

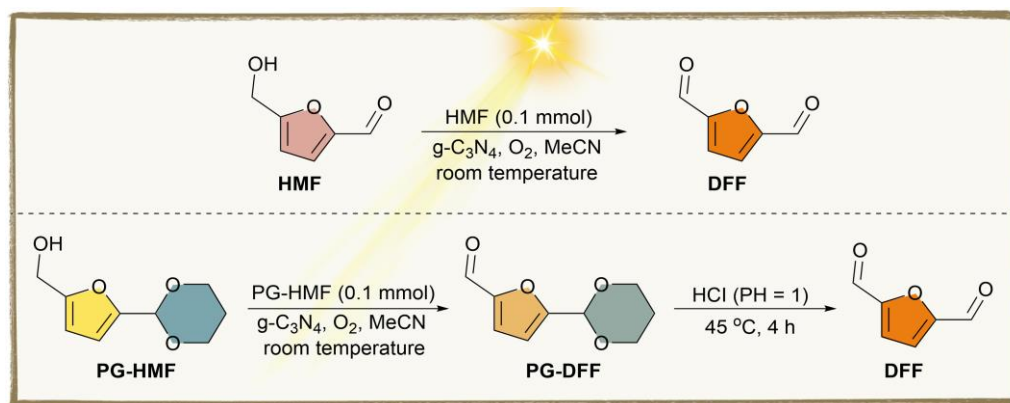
potential for applications such as advanced fuel additives.

Protection group effect in photocatalytic oxidation reactions

Finally, we evaluate the reactivity of HMF before or after protecting the C=O group in photocatalytic oxidation over some representative photocatalysts (Table 3). Non-selective TiO₂ is not suitable for the photo-oxidation due to the excessive oxidation of the target product (Table S2). Thus, g-C₃N₄ is further employed. In the presence of light at a wavelength of 467 nm and oxygen for 12 h, the DFF selectivity achieved 19.6%

at 62.6% conversion of HMF (entry 1). After protecting the C=O group, the selectivity of 2,5-diformylfuran acetal (PG-DFF) increased to 37.1% (entry 2). Under irradiation at 427 nm for 3 h, the yield of DFF was improved to 21.4% with a selectivity of 25.7%. When the time was extended to 12 h, the yield of DFF significantly decreased to 5.5% (entries 3 and 4). After protecting the C=O group, the selectivity of the target product significantly improved (entries 5 and 6). Specifically, more oxidative products can be retained after 12 h, confirming that

Table 3. Protection group effect in photocatalytic oxidation over g-C₃N₄ catalyst.^a



Entry	Substrate	Incident light/nm	t	Conv./%	Yield/%		Sel./%
					DFF	PG-DFF	
1	HMF	467	12	62.6	12.3	-	19.6
2	PG-HMF	467	12	55.5	-	20.6 (20.0) ^b	37.1
3	HMF	427	3	83.3	21.4	-	25.7
4	HMF	427	12	>99.9	5.5	-	5.51
5	PG-HMF	427	3	64.3	-	26.2 (25.4) ^b	40.7
6	PG-HMF	427	12	99.7	-	22.7 (22.0) ^b	22.7

^a Reaction conditions: 0.1 mmol substrate, 50 mg photocatalyst, $\lambda = 467$ or 427 nm, 40 W, room temperature, O₂ balloon, 3 mL CH₃CN. ^b The DFF yield generated from PG-DFF deprotection is shown in parentheses.

the protection of C=O bond can significantly suppress side reactions. The deprotection of PG-DFF can be realized at 45 °C for 4 h using HCl aqueous solution (pH = 1), giving 97% conversion of PG-DFF and >99.9% selectivity of DFF (entry 2 and entries 5-6). Some other photocatalysts such as Cd_{1.5}In₂S_{4.5} catalyst is also examined, but the selectivity of products is quite low (Table S2). Novel photocatalytic materials should be further fabricated to improve the photocatalytic selectivity and efficiency, which are ongoing in our lab.

Conclusions

The protection strategy has shown great potential to improve the selectivity and efficiency during biomass conversion such as lignin depolymerization, sugar production, and platform chemical conversions. Here we focus on the exploration of such strategy for the conversion of perhaps most important biomass-based platform chemicals, the furanic aldehydes. An efficient, column chromatography-free route for the scale-up preparation of acetals is first established to afford g-grade, high-purity acetal products. Issues such as waste of eluent and time, inability of separating biomass-based substrates of strong polarity, and potential deprotection during eluting that lowers the final purity in traditional purification via column chromatography are overcome. Then we explore the protection group effect in hydrodeoxygenation (HDO), ring hydrogenation, and photocatalytic systems using MF, HMF furfural and their corresponding acetals as model compounds. The protective effect in HDO is not as significant as previous reports about aerobic oxidation, likely due to the different reaction pathways and active sites. In addition, HDO, deoxygenation (DO), or ring hydrogenation became dominant pathways over carbon, Al₂O₃, MgO- supported catalysts, respectively, probably due to their different acidic or basic properties. Furthermore, the acetals obtained after selective hydrogenation of the furanic ring exhibited better stability under acidic environment, suggesting that they are promising fuel additives. Finally, the protection strategy is found to be effective in photocatalytic oxidation of HMF with 2-4 times higher selectivity. Overall, our work paves the way for future exploration of the protection strategy in (photo)-chemical biomass conversion.

Experimental

Materials

HMF was provided as a gift from Hefei Leaf Energy Biotechnology Co., Ltd. Trifluoromethanesulfonic acid (TFA, 98%), sulfuric acid (SA, 98%), p-toluenesulfonic acid (PTSA, 99%), methanesulfonic acid (MSA, 99%), sulfamic acid (SFA, 99.5%), sodium hydrogen sulfate (SHS, 95%), citric acid (CTA, 99.5%), boric acid (BA, 99.5%), melamine (99%), TiO₂, anatase, P25, thioacetamide (TAA, 99%), Indium nitrate hydrate (99.9%), Cadmium nitrate tetrahydrate (Ar, 99%) and ferric acetylacetonate (98%) were purchased from Aladdin Reagent Co. Ltd. Magnesium oxide (98%), aluminium oxide (98%), ethyl

acetate (99.5%), magnesium sulfate anhydrous (95%), furfural (98%), 1,3-propylene glycol (98%), MF (97%), DMF (98%), 1,10-phenanthroline monohydrate (99%) and activated carbon were purchased from TCI. CH₃CN (>99.9%, HPLC grade purity), Dichloromethane (99.9%) were purchased from PUREDIL chemicals Co. Ltd. NaCl (99.5 wt%) were purchased from Tianjin Fuchen Chemical Reagent Co. Ltd. THF (99%), n-hexane (98%), p-xylene (98%) and toluene (99.5%) were purchased from Beijing Chemical Reagent Co. Ltd. RuCl₃ (99.9%, Ru 37%) were purchased from Shanghai Jiuling Chemical Reagent Co. Ltd. and Amberlyst-15(H⁺ content: 4.6-4.8 mmol·g⁻¹) were purchased from Chengdu Aikeda Chemical Reagent Co. Ltd.

Catalyst preparation

The Fe-phen/C-800 and Fe-phen/Al₂O₃-800 catalyst is prepared as in our previous work.^{40,44} To improve the Fe catalysts' hydrogenation activity, a RuFe bimetallic catalyst and Ru-280-MgO catalyst were prepared via wetness impregnation. 1 g Fe-phen/C-800, Fe-phen/Al₂O₃-800 catalyst and 1 g MgO were first mixed with 50 mL ethanol solution of RuCl₃ (27.1 mg) at 50 °C for 4 h. Then the catalysts were dried by rotary evaporation at 30 °C and reduced under 5% H₂/Ar in a tubular furnace using the following temperature program: 30 °C (60 min) followed by a ramp of 1 °C/min to 280 °C, and then hold for another 2 h.

G-C₃N₄ was synthesized by the self-condensation of melamine.⁴⁵ In a typical synthesis, 10 g of melamine is added into a covered ceramic crucible, and then heated under Ar at 550 °C for 2 h at a heating rate of 2 °C/min. The resulting product was ground into powder to afford the g-C₃N₄ catalyst.

Cd_{1.5}In₂S_{4.5} was prepared by one-step hydrothermal method.⁴⁶ Typically, 0.34 g TAA were successively dissolved in 70 mL deionized water under continuous stirring. Then, 0.46 g Cd(NO₃)₂·4H₂O and 0.64 g In(NO₃)₃·4H₂O were added into the above solution. After stirring for 30 min, the solution was transferred into a 100 mL Teflon-lined autoclave and heated at 180 °C for 20 h. Finally, the precipitate was washed with ethanol and deionized water for several times and dried at 60 °C in a vacuum oven to give Cd_{1.5}In₂S_{4.5} composites.

Catalyst characterization

For NH₃- and CO₂-TPD tests, approximately 100 mg of the sample was loaded in a quartz reactor and then heated at 500 °C under argon flow for 2 h. Then the adsorption of NH₃ or CO₂ was carried out at 40 °C for 1 h. Subsequently, the catalysts were flushed with argon for another 1 h and then heated to 800 °C with a heating ramp rate of 10 °C·min⁻¹. The desorbed NH₃ or CO₂ was measured by a gas chromatograph equipped with a thermal conductivity detector (TCD).

Experimental procedure

To examine the effect of pKa, 1 mmol acid catalyst was added to the mixture of furfural (1 mmol), 1,3-propylene glycol (1 mmol), and dichloromethane solvent (3 mL). The mixture was stirred at 30 °C for 3 h. After reaction, the internal standard toluene was added, and the liquid products were analyzed using both GC and GC-MS. The reaction temperature, catalyst

loading, and the ratio of furfural and 1,3-propylene glycol varied as noted in figure captions.

For scale-up of acetal production, 1 mmol sulfamic acid, 10 mmol furfural, 40 mmol 1, 3-propandiol, and 60 mL dichloromethane solvent were added into a glass flask, and the mixture was heated to 60 °C for 6 h. The reaction conditions for MF and HMF are 80 °C, 6 h and 25 °C, 0.5 h, respectively. For high-concentration scale-up preparation of HMF-derived acetals, 5 mmol SFA, 50 mmol HMF, 200 mmol 1, 3-propandiol, and 100 mL dichloromethane solvent were added into a glass flask. Then the mixture was heated to 25 °C for 2 h. The reaction conditions for high-concentration scale-up of furfural-based acetals are operated at 60 °C for 6 h. After cooling to room temperature, the acid catalyst was separated first via filtration and then saturated brine was used for extraction for three times. After extraction, the organic phase was dried by anhydrous magnesium sulfate. The acetal products are finally obtained by removing the anhydrous magnesium sulfate followed by rotary evaporation.

For the preparation of PG-DFF, 0.3 mmol SFA, 1 mmol DFF, 2 mmol 1, 3-propandiol, and 6 mL dichloromethane solvent were added into a glass flask, and then the mixture was heated to 25 °C for 8 h. Preparative thin-layer chromatography (PTLC) is employed to purify PG-DFF from the reaction mixture using dichloromethane and ethyl acetate as elution solvents. The colored product under UV light was scraped off and transferred into a glass flask. It was then dissolved in a small amount of dichloromethane, filtered, and obtained as the purified PG-DFF product (Figures S14-15). PG-THFFA was obtained from ring hydrogenation of furfural. After reaction, heterogeneous Ru-280-MgO catalyst was removed via filtration, and then the solvent in percolate was removed by rotating evaporation at 40 °C (see NMR spectrum in Figure S16). ¹H NMR and GC spectra of the acetals were recorded using a nuclear magnetic resonance spectrometer (JNM-ECA600) and an Agilent 7890 Gas Chromatograph, respectively.

To examine the protection group effect, the reactivity of aldehydes and corresponding acetals are compared in HDO. 0.5 mmol substrate is used in low-concentration experiments, and 5 or 20 mmol substrate is used in high-concentration experiments. In a typical HDO experiment, 100 mg Fe-phen/C-800 or 1%Ru-Fe-phen/C-800 catalysts, 0.5 mmol HMF or PG-HMF, and 20 mL THF solvent were loaded into a 50 mL Zr-alloy autoclave provided by Anhui Kemi Instrument Co., LTD. After purging with 4 MPa H₂, the reactor was heated to 240 °C for 12 h, followed by cooling and washing to obtain the product liquid. The ring hydrogenation was typically operated at 160 °C for 2 h under 4 MPa H₂. Toluene was added as an internal standard, and the sample was analyzed using an Agilent 7890 Gas Chromatograph.

The photocatalytic reaction was carried out in a glass tube equipped with a glass valve to exchange the atmosphere (10 mL capacity, Synthware). In a typical reaction, 0.1 mmol HMF or PG-HMF, 50 mg g-C₃N₄, and 3 mL acetonitrile were added into the glass tube. Then the atmosphere was changed to oxygen, and an O₂ balloon is equipped. The mixture was irradiated by a 40W blue LED lamp (kessil, PR160L, λ = 467 nm) or 300W Xe lamp

(Perfectlight, PLS-SXE300, λ = 320-780 nm) with air cooling, and the distance between the light source and the reactor wall is about 2 mm. After the reaction, the reaction solution was collected and toluene was added as the internal standard. The deprotection of PG-DFF after the photo-oxidation can be realized at 45 °C for 4 h with HCl aqueous solution (pH = 1). The products were analyzed by gas chromatography (GC) and gas chromatography-mass spectrometry (GC-MS).

The stability reaction was carried out in a 50 mL glass flask (Figure 2). For a typical reaction, 0.25 mmol PG-FFA and 2 mL 0.01 mol/L HCl aqueous solution were added into the flask, and the mixture was stirred at room temperature. Then, it is neutralized with a 0.05 mol/L NaOH aqueous solution. P-xylene (PX) was added as an internal standard, and the reaction mixture is diluted with an organic solvent (such as acetonitrile). The deprotection conversion was analyzed using GC. The stability test of PG-THFFA was performed as follows: Firstly, the reaction mixture (0.5 mmol) was divided into two parts. One part (0.25 mmol) is used to quantify the amount of PG-THFFA and PG-FFA in the mixture by adding p-xylene as an internal standard. The other part was subjected to deprotection as the deprotection of PG-FFA described above after removal of solvent by rotary evaporation.

The conversion, yield, and selectivity of acetalization and HDO are calculated as on a molar basis:

Conversion

$$= \left(1 - \frac{\text{molar amount of substrate after reaction}}{\text{molar amount of substrate before reaction}} \right) * 100\%$$

$$\text{Yield} = \frac{\text{molar amount of product after reaction}}{\text{molar amount of substrate before reaction}} * 100\%$$

$$\text{Selectivity} = \frac{\text{Yield of product}}{\text{Conversion of substrate}} * 100\%$$

Author Contributions

J. Li and D. G. Vlachos designed the study and wrote the paper. L. Huang, C. Li, and H. Q. Zhang conduct an investigation, data collection, visualization, writing- original draft preparation. Z. D. An revised the paper.

Conflicts of interest

There are no conflicts to declare.

Acknowledgements

LH, CL, ZA, HZ, and JL were supported by the National Key R&D Program of China (Grant No. 2022YFB3506200), National Natural Science Foundation of China (21702227, 22122113), Science Foundation of China University of Petroleum, Beijing (No. 2462014YJRC037). DGV acknowledge support from the Catalysis Center for Energy Innovation, an Energy Frontier Research Center funded by the U.S. Department of Energy, Office of Science, Office of Basic Energy Sciences under Award

number DE-SC0001004. Dr. Jiang Li also thanks the support of the China Scholarship Council (CSC).

Notes and references

- S. I. George W. Huber, and Avelino Corma, *Chem. Rev.*, 2006, **106**, 4044-4098.
- D. R. Dodds and R. A. Gross, *Science*, 2007, **318**, 1250-1251.
- L. D. S. a. P. J. Dauenhauer, *Nature*, 2007, **447**, 914-915.
- S. I. Avelino Corma, and Alexandra Velty, *Chem. Rev.*, 2007, **107**, 2411-2502.
- K. I. Galkin, E. A. Krivodaeva, L. V. Romashov, S. S. Zaleskiy, V. V. Kachala, J. V. Burykina and V. P. Ananikov, *Angew. Chem. Int. Ed.*, 2016, **55**, 8338-8342.
- M. Talebi Amiri, G. R. Dick, Y. M. Questell-Santiago and J. S. Luterbacher, *Nat. Protoc.*, 2019, **14**, 921-954.
- S. Li, M. T. Amiri, Y. M. Questell-Santiago, F. Héroguel, Y. Li, H. Kim, R. Meilan, C. Chapple, J. Ralph and J. S. Luterbacher, *Science*, 2016, **354**, 329-333.
- W. Lan, M. T. Amiri, C. M. Hunston and J. S. Luterbacher, *Angew. Chem. Int. Ed.*, 2018, **57**, 1356-1360.
- W. Lan, J. B. de Bueren and J. S. Luterbacher, *Angew. Chem. Int. Ed.*, 2019, **58**, 2649-2654.
- J. Behaghel de Bueren, F. Héroguel, C. Wegmann, G. R. Dick, R. Buser and J. S. Luterbacher, *ACS Sustain. Chem. Eng.*, 2020, **8**, 16737-16745.
- R. Vendamme, J. Behaghel de Bueren, J. Gracia-Vitoria, F. Isnard, M. M. Mulunda, P. Ortiz, M. Wadekar, K. Vanbroekhoven, C. Wegmann, R. Buser, F. Heroguel, J. S. Luterbacher and W. Eevers, *Biomacromolecules*, 2020, **21**, 4135-4148.
- Y. M. Questell-Santiago, R. Zambrano-Varela, M. Talebi Amiri and J. S. Luterbacher, *Nat. Chem.*, 2018, **10**, 1222-1228.
- Y. M. Questell-Santiago, J. H. Yeap, M. Talebi Amiri, B. P. Le Monnier and J. S. Luterbacher, *ACS Sustain. Chem. Eng.*, 2020, **8**, 1709-1714.
- M. Kim, Y. Su, A. Fukuoka, E. J. M. Hensen and K. Nakajima, *Angew. Chem. Int. Ed.*, 2018, **57**, 8235-8239.
- M. Kim, Y. Su, T. Aoshima, A. Fukuoka, E. J. M. Hensen and K. Nakajima, *ACS Catal.*, 2019, **9**, 4277-4285.
- T. Boonyakarn, J. J. Wiesfeld, M. Asakawa, L. Chen, A. Fukuoka, E. J. M. Hensen and K. Nakajima, *ChemSusChem*, 2022, **15**, e202200059.
- J. J. Wiesfeld, M. Asakawa, T. Aoshima, A. Fukuoka, E. J. M. Hensen and K. Nakajima, *ChemCatChem*, 2022, **14**, e202200191.
- J. J. Wiesfeld, M. Kim, K. Nakajima and E. J. M. Hensen, *Green Chem.*, 2020, **22**, 1229-1238.
- Y. M. Questell-Santiago, M. V. Galkin, K. Barta and J. S. Luterbacher, *Nat. Rev. Chem.*, 2020, **4**, 311-330.
- X. Luo, Y. Li, N. K. Gupta, B. Sels, J. Ralph and L. Shuai, *Angew. Chem. Int. Ed.*, 2020, **59**, 11704-11716.
- W. Lan and J. S. Luterbacher, *Chimia (Aarau)*, 2019, **73**, 591-598.
- W. Lan, M. T. Amiri, C. M. Hunston and J. S. Luterbacher, *Angew. Chem. Int. Ed.*, 2018, **57**, 1356-1360.
- F. J. A. G. Coumans, Z. Overchenko, J. J. Wiesfeld, N. Kosinov, K. Nakajima and E. J. M. Hensen, *ACS Sustain. Chem. Eng.*, 2022, **10**, 3116-3130.
- Y. Nakagawa, M. Tamura and K. Tomishige, *ACS Catal.*, 2013, **3**, 2655-2668.
- L. Hu, L. Lin, Z. Wu, S. Zhou and S. Liu, *Renew. Sust. Energ. Rev.*, 2017, **74**, 230-257.
- S. Chen, R. Wojcieszak, F. Dumeignil, E. Marceau and S. Royer, *Chem. Rev.*, 2018, **118**, 11023-11117.
- H. Wang, C. Zhu, D. Li, Q. Liu, J. Tan, C. Wang, C. Cai and L. Ma, *Renew. Sust. Energ. Rev.*, 2019, **103**, 227-247.
- X. Kong, Y. Zhu, Z. Fang, J. A. Kozinski, I. S. Butler, L. Xu, H. Song and X. Wei, *Green Chem.*, 2018, **20**, 3657-3682.
- H. C. R. G. Cooks, Marcos N. Eberlin, Xubin Zheng and W. Andy Tao, *Chem. Rev.*, 2006, **106**, 188-211.
- S. Kanai, I. Nagahara, Y. Kita, K. Kamata and M. Hara, *Chem. Sci.*, 2017, **8**, 3146-3153.
- M. J. da Silva and M. G. Teixeira, *Mol. Catal.*, 2018, **461**, 40-47.
- J. M. Rubio-Caballero, S. Saravanamurugan, P. Maireles-Torres and A. Riisager, *Catal. Today*, 2014, **234**, 233-236.
- M. Nagao, S. Misu, J. Hirayama, R. Otomo and Y. Kamiya, *ACS Appl. Mater. Interfaces*, 2020, **12**, 2539-2547.
- Y. Du, X. Liu, X. Wu, Q. Cheng, C. Ci and W. Huang, *ChemistrySelect*, 2018, **3**, 7996-8002.
- M. J. da Silva, M. G. Teixeira and R. Natalino, *New J. Chem.*, 2019, **43**, 8606-8612.
- N. Castellanos - Blanco, G. Taborda and M. Cobo, *ChemistrySelect*, 2020, **5**, 3458-3470.
- K. S. Arias, A. Garcia-Ortiz, M. J. Climent, A. Corma and S. Iborra, *ACS Sustain. Chem. Eng.*, 2018, **6**, 4239-4245.
- X. Hu, R. J. M. Westerhof, D. H. Dong, L. P. Wu and C. Z. Li, *ACS Sustain. Chem. Eng.*, 2014, **2**, 2562-2575.
- J. Li, D. Ding, L. Xu, Q. Guo and Y. Fu, *RSC Adv.*, 2014, **4**, 14985-14992.
- J. Li, J. L. Liu, H. Y. Liu, G. Y. Xu, J. J. Zhang, J. X. Liu, G. L. Zhou, Q. Li, Z. H. Xu and Y. Fu, *ChemSusChem*, 2017, **10**, 1436-1447.
- B. L. Wegenhart, S. Liu, M. Thom, D. Stanley and M. M. Abu-Omar, *ACS Catal.*, 2012, **2**, 2524-2530.
- B. Malleshham, P. Sudarsanam, G. Raju and B. M. Reddy, *Green Chem.*, 2013, **15**, 478-489.
- A. Patil, S. Shinde, S. Kamble and C. V. Rode, *Energy Fuels*, 2019, **33**, 7466-7472.
- J. Li, J. Liu, H. Zhou and Y. Fu, *ChemSusChem*, 2016, **9**, 1339-1347.
- I. Krivtsov, E. I. García-López, G. Marci, L. Palmisano, Z. Amghouz, J. R. García, S. Ordóñez and E. Díaz, *Appl. Catal. B: Environ.*, 2017, **204**, 430-439.
- M. Zhang, Z. Yu, J. Xiong, R. Zhang, X. Liu and X. Lu, *Appl. Catal. B: Environ.*, 2022, **300**, 120738.